Nonlinear Dyn (2009) 58: 217–235
DOI 10.1007/s11071-009-9473-4

ORIGINAL PAPER

Explicit dynamics equations of the constrained robotic systems

Stefan Staicu · Xin-Jun Liu · Jianfeng Li

Received: 26 February 2008 / Accepted: 26 January 2009 / Published online: 18 February 2009

Abstract Recursive matrix relations concerning the kinematics and the dynamics of a constrained robotic system, schematized by several kinematical chains, are established in this paper. Introducing frames and bases, we first analyze the geometrical properties of the mechanism and derive a general set of relations. Kinematics of the vector system of velocities and accelerations for each element of robot are then obtained. Expressed for every independent loop of the robot, useful *conditions of connectivity* regarding the relative velocities and accelerations are determined for direct or inverse kinematics problem. Based on the general principle of virtual powers, final matrix relations written in a recursive compact form express just the *explicit dynamics equations* of a constrained robotic system. Establishing active forces or actuator torques in an inverse dynamic problem, these equations are useful in fact for real-time control of a robot.

Keywords Dynamics · Kinematics · Parallel robot · Virtual power

List of symbols

$a_{k,k-1}$	orthogonal relative transformation matrix
a	general transformation matrix of moving platform
$\vec{u}_1, \vec{u}_2, \vec{u}_3$	three orthogonal unit vectors
$\varphi_{k,k-1}$	relative rotation angle of T_k rigid body
$\vec{\omega}_{k,k-1}$	relative angular velocity of T_k
$\vec{\omega}_{k0}$	absolute angular velocity of T_k
$\tilde{\omega}_{k,k-1}$	skew symmetric matrix associated with the angular velocity $\vec{\omega}_{k,k-1}$
$\vec{\varepsilon}_{k,k-1}$	relative angular acceleration of T_k
$\tilde{\varepsilon}_{k0}$	absolute angular acceleration of T_k
$\tilde{\varepsilon}_{k,k-1}$	skew symmetric matrix associated with the angular acceleration $\vec{\varepsilon}_{k,k-1}$
$\vec{r}^{\,A}_{k,k-1}$	relative position vector of the center A_k of joint
$\vec{v}^{\,A}_{k,k-1}$	relative velocity of the center A_k
$\vec{\gamma}^{\,A}_{k,k-1}$	relative acceleration of the center A_k
m_k	mass of T_k rigid body
$\hat{J}_k$	symmetric matrix of tensor of inertia of T_k about the link-frame $A_k x_k y_k z_k$
$f_{q,q-1}, m_{q,q-1}$	force or torque of the actuator T_{q-1}

S. Staicu
Department of Mechanics, University "Politehnica" of Bucharest, Bucharest, Romania

X.-J. Liu (✉)
Institute of Manufacturing Engineering, Department of Precision Instruments, Tsinghua University, Beijing 100084, China
e-mail: xinjunliu@mail.tsinghua.edu.cn

J. Li
The College of Mechanical Engineering & Applied Electronics Technology, Beijing University of Technology, Beijing 100022, China

1 Introduction

Parallel robots are planar or spatial closed-loop mechanisms presenting high speed, greater rigidity and ability to manipulate large loads.

Generally, this kind of robots consists of two significant bodies coupled by several legs. One body is arbitrarily designated as fixed and is called *base*, while the other is connected by several legs to the fixed base and is called *moving platform*. The elements of the robot are connected one to the other by spherical joints, revolute joints or prismatic joints. Typically, a parallel mechanism is said to be *symmetrical* if it satisfies the following conditions: the number of legs is equal to the number of degree of freedom (DOF) of the moving platform, one actuator controls every limb and the location and the number of actuated joints in all the limbs are the same (Tsai [1]).

For two decades, parallel robots attracted the attention of many researches that consider them as valuable alternative design for robotic mechanisms [2, 3]. Other types of architecture [4] have therefore recently been studied, and are being more and more regularly used within the industrial world such as machine tools [5] and industrial robots [6]. Parallel robots can be found in technical applications in which it is desired a high-speed displacement of a rigid body in space. Accuracy and precision in the execution of the tasks are essential since the robot is intended to operate on fragile objects; any error in the positioning of the tool could lead to expensive damage.

Parallel robots could be equipped with hydraulic or pneumatic actuators. They have a robust construction and can move bodies of considerable masses and dimensions with high speeds. This is why the mechanisms, which produce a translation or spherical motion to a platform, are based on the concept of parallel robot.

Compared with the serial robots, parallel robots have some special characteristics: greater structural rigidity, stable functioning, larger dynamic charge capacity and suitable position of the actuating systems. On the other hand, parallel kinematics machines offer essential advantages over their serial counterparts: lower moving masses, higher natural frequencies, simpler modular mechanical construction and possibility to mount all actuators at or near the fixed base. However, most existing parallel robots have a limited and complicated workspace volume with singularities and highly non-isotropic input–output relations [7, 8].

Recently, much effort has been devoted to the kinematics studies and dynamics analysis in parallel robots and hybrid serial and parallel architecture. Many companies have developed them as high precision machine tools. The class of robots known as Stewart platform focussed great attention (see [7, 9, 10]). They are used in flight simulators and more recently for parallel kinematical machines. The prototype of Delta parallel robot [11, 12], Tsai's mechanism [13], as well as the Star parallel robot [14], are equipped with three actuators and move its platforms in a three-degrees-of-freedom general translation. Gosselin and Angeles [15] developed the direct kinematics and dynamics of the Agile Wrist spherical parallel robot, which has three concurrent rotations.

The kinematics of parallel robots has been studied extensively during the last two decades. When good dynamic performance and precise positioning under high load are required, the dynamic model is important for their control. The dynamic analysis of parallel robots is usually implemented through analytical methods in classical mechanics [16], in which projection and resolution of equations on the reference axes are written in a considerable number of cumbersome, scalar relations and the solutions are rendered by large scale computation together with time consuming computer codes.

Many works have been focussed on the dynamics of Stewart platform. Dasgupta and Mruthyunjaya [17] used the Newton–Euler approach to develop closed-form dynamical equations of Stewart platform, considering all dynamic and gravity effects as well as viscous friction at joints. Tsai [1] presented also an algorithm to solve the inverse dynamics for a Stewart platform, using Newton–Euler procedure. It is commonly known that this approach results in an efficient set of equations, but they are very difficult to use for deriving of the advanced control laws.

Meanwhile, quite few of special approaches have been conducted for dynamic modeling of specific parallel mechanism configurations. Kane and Levinson [18] obtained some recursive relations concerning the equilibrium of the generalized forces that are applied to a serial robot arm. Kane's dynamical equations are described with an example of Stanford robot, and they did not propose a general algorithm for constrained robotic systems. Sorli et al. [19] conducted the dynamics modeling for Turin parallel robot, which has three identical legs but 6 DOFs.

Under some simplifying assumptions on the geometry and inertia distribution of the robot, Geng et al. [20] and Tsai and Stamper [13] developed the Lagrange formalism in equations of motion. The analytical calculi involved in the Lagrange method are too long for every scheme of robots and they have error risk. Also, it is proved that the time for numerical calculus grows with the number of bodies in the robotic systems. Computationally, it is impossible to utilize this elegant approach for real-time command, unless the numerous final equations are simplified.

Recursive matrix relations for the kinematics and the dynamics of a general constrained robotic system, schematized by closed kinematical chains, are established in this paper. Based on the general principle of virtual powers, final matrix relations written in a recursive compact form express just the *explicit dynamics equations of a constrained robotic system*.

The methodology developed in this paper can be available for kinematics analysis and nonlinear dynamics of a multi-body systems consisting of interconnected rigid and, eventually, deformable bodies, each of which may undergo large translation and rotational displacements. Examples of mechanical structures that can be modeled as constrained robotic systems are: mechanisms, machines, parallel robots, mobile robots, gear trains for robotics and spatial robotic hybrid architectures.

2 Geometric model of the robot

Generally, a serial leg of a robot consists of a base link T_0 and n movable links connected by N joints. The kinematical joints constrain the virtual position of the mechanism and transmit the relative motion from one body to the other.

To describe the geometry of links, starting from the base link T_0 we number the movable links sequentially from T_1 to T_n and the joints from O_1 to O_N. Thus, except for the base link, every link has two joints; the link T_k has the joint O_k at its proximal end and the joint O_{k+1} at the distal end.

We now introduce several frames. First, the fixed frame $O_0 - x_0 y_0 z_0$ is attached to the base T_0 at a convenient location. Consider the set of moving bodies T_k $(k = 1, 2, \ldots, n)$ attached to the moving frames $O_k - x_k y_k z_k$. Along the z_k-axis, an arbitrary T_k body has a relative helical motion with respect to T_{k-1} (see Fig. 1). A combination of translation along and rotation about the same axis is called *screw displacement* (Tsai [1]).

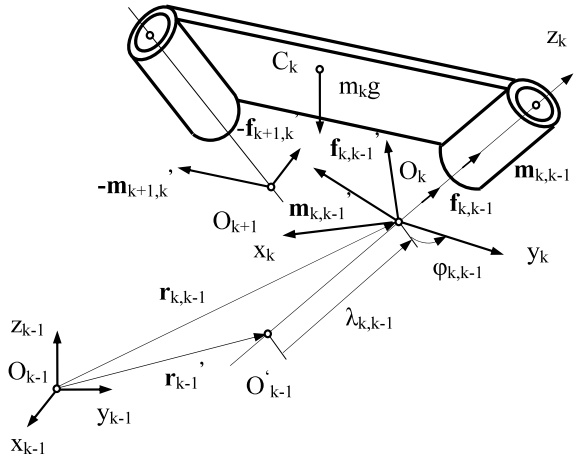

Fig. 1 Geometry and forces exerted on link T_k

In what follows we apply the concept of successive screw displacements to geometrical analysis of closed-loop chains and we note that a *joint variable* is the displacement required to move a link from initial location to actual position. But, a variable associated to an active joint is denoted as input variable of active joint.

The geometric parameters describing the relative position of T_k with respect to adjacent link T_{k-1} shall be uniquely determined: the translation displacement $O'_{k-1}O_k = \lambda_{k,k-1}$ of the origin O_k and the joint angle $\varphi_{k,k-1}$ of rotation about the positive z_k-axis according to the right-hand rule. These variables represent in fact the distance of translation and the angle of rotation needed to bring a link from its reference configuration to the next configuration and should not be confused with the Denavit–Hartenberg parameters [1, 7]. But, their relation to the D–H parameters can be derived from these two coordinates by creating relative displacements with respect to the reference configuration and performing some simple matrix operations [21].

Linked to rigid body T_k, the moving frame $O_k - x_k y_k z_k$ makes either translation, rotation or simultaneously a complex motion of rotation-translation along the common axis z_x of the connecting joint between the two adjacent bodies T_k and T_{k-1}. Any vector or tensor is expressed by its components about the axes of the attached frame $O_k - x_k y_k z_k$.

For a revolute joint the displacement $\lambda_{k,k-1}$ is constant and the angle $\varphi_{k,k-1}$ is a variable that measures

the relative rotation of link T_k with respect to the near link T_{k-1}. For a prismatic joint, $\varphi_{k,k-1}$ is constant and $\lambda_{k,k-1}$ is a variable that measures the relative translation between two links. We note that a universal joint can be modeled by two intersecting revolute joints and that for a spherical joint three successive rotations about three orthogonal concurrent axes can be considered.

The two independent coordinates, $\lambda_{k,k-1}$ and $\varphi_{k,k-1}$, determine the position of the vector

$$\vec{r}_{k,k-1} = \vec{r}'_{k-1} + \lambda_{k,k-1} a^T_{k-1} \vec{u}_3, \quad \vec{u}_3 = [0 \quad 0 \quad 1]^T \tag{1}$$

and give the variable orthogonal transformation 3×3 matrix $a^{\varphi}_{k,k-1}$ for relative rotation of link T_k around the z_k-axis, where

$$\vec{r}_{k,k-1} = \begin{bmatrix} x_{k,k-1} \\ y_{k,k-1} \\ z_{k,k-1} \end{bmatrix},$$

$$\overrightarrow{O_{k-1}O'_{k-1}} = \vec{r}'_{k-1} = \begin{bmatrix} x'_{k-1} \\ y'_{k-1} \\ z'_{k-1} \end{bmatrix}, \tag{2}$$

$$a^{\varphi}_{k,k-1} = \begin{bmatrix} \cos\varphi_{k,k-1} & \sin\varphi_{k,k-1} & 0 \\ -\sin\varphi_{k,k-1} & \cos\varphi_{k,k-1} & 0 \\ 0 & 0 & 1 \end{bmatrix}.$$

The above matrix product $a_{k-1} = a^{\theta}_{k-1} a^{\psi}_{k-1}$ of two constant orthogonal matrices, a^{θ}_{k-1} and a^{ψ}_{k-1}, allows expressing any vector and tensor from frame T_{k-1} to the next frame which is fixed at O'_{k-1} in the same rigid body [21, 22]:

$$a^{\theta}_{k-1} = \begin{bmatrix} \cos\theta_{k-1} & 0 & -\sin\theta_{k-1} \\ 0 & 1 & 0 \\ \sin\theta_{k-1} & 0 & \cos\theta_{k-1} \end{bmatrix},$$

$$a^{\psi}_{k-1} = \begin{bmatrix} \cos\psi_{k-1} & \sin\psi_{k-1} & 0 \\ -\sin\psi_{k-1} & \cos\psi_{k-1} & 0 \\ 0 & 0 & 1 \end{bmatrix}. \tag{3}$$

Now, the position of the permanent axis of relative helical motion is completely determined by the constant vector $\vec{r}'_{k-1}$ and the constant matrix a_{k-1}. After one translation and two orthogonal rotations followed by one relative rotation or translation about z_x-axis, a change of coordinates between T_{k-1} and T_k frames is completely given by the relations (1), (2), (3). If every link is connected to at least two other links, finally the chain forms one or more independent closed-loops.

Some matrix equations, relating the location of a link T_σ and the position of the end-effector to the independent joint variables, should be expressed in a geometrical modeling of robot systems. Recursive form of position vector for origin O_σ

$$\begin{aligned} &\vec{r}_{\sigma s} = \vec{r}_{\sigma-1,s} + a^T_{\sigma-1,s} \vec{r}_{\sigma,\sigma-1}, \\ &\vec{r}_{ss} = \vec{0}, \qquad a_{ss} = I, \qquad \sigma \geq s+1 \end{aligned} \tag{4}$$

and following transformation matrices [23]

$$\begin{aligned} a_{\sigma s} &= \prod_{j=1}^{\sigma-s} a_{\sigma-j+1,\sigma-j}, \\ a^T_{\sigma s} &= \prod_{j=s+1}^{\sigma} a^T_{j,j-1}, \quad a_{j,j-1} = a^{\varphi}_{j,j-1} a_{j-1} \end{aligned} \tag{5}$$

can give the relative position of the link T_σ in the frame T_s. When the change of coordinates is taken in succession, the corresponding matrices are multiplied. These can be thought of as the resultant of a series of coordinate transformations, starting from base T_s and ending at link T_σ.

In the forward kinematics, the joint variables are given and the problem is to find where the end-effector is with respect to the base coordinate system. In the inverse kinematics, the position of end-effector is given. Here, the problem is to compute the joint displacements needed to bring the end-effector to the desired location.

If the reference point in the movable platform T_n is located at its center G, the location of T_n with respect to $O_0 - x_0 y_0 z_0$ can be described along every leg by the position vector $\vec{r}^{\,G}_0$ of the origin G and the absolute rotation matrix a_{n0} as follows:

$$\begin{aligned} \vec{r}^{\,G}_0 &= \vec{r}_{10} + \sum_{k=1}^{n-1} a^T_{k0} \vec{r}_{k+1,k} + a^T_{n0} \vec{r}^{\,G}_n, \\ a_{n0} &= \prod_{k=1}^{n} a_{n-k+1,n-k}. \end{aligned} \tag{6}$$

These loop-closure equations constitute the *geometrical model* of a parallel robot. Generally, the number of the relations that can be established for a mechanism is equal to the number of independent closed-loops.

3 Velocities and accelerations

Relative helical motion of the T_k link of the robot is determined by the linear relative velocity $\vec{v}_{k,k-1}$ of the origin O_k and by the angular velocity vector $\vec{\omega}_{k,k-1}$:

$$\vec{v}_{k,k-1} = \dot{\lambda}_{k,k-1}\vec{u}_3, \qquad \vec{\omega}_{k,k-1} = \dot{\varphi}_{k,k-1}\vec{u}_3. \tag{7}$$

We note that a very useful skew-symmetric matrix 3×3 *associated* to vector $\vec{\omega}_{k,k-1}$ is obtained:

$$\tilde{\omega}_{k,k-1} = a_{k,k-1}\dot{a}^T_{k,k-1} = \dot{\varphi}_{k,k-1}\tilde{u}_3,$$
$$\tilde{u}_3 = \begin{bmatrix} 0 & -1 & 0 \\ 1 & 0 & 0 \\ 0 & 0 & 0 \end{bmatrix}, \qquad \det\tilde{\omega}_{k,k-1} = 0. \tag{8}$$

To describe the kinematical state of each link T_σ with respect to T_s frame, we compute the angular velocity $\vec{\omega}_{\sigma s}$ and the linear velocity $\vec{v}_{\sigma s}$ of the reference point O_σ in terms of vectors of preceding body. Starting from the first moving link T_s and ending at last link T_σ, both vectors can easily be expressed in a recursive manner:

$$\vec{v}_{\sigma s} = a_{\sigma,\sigma-1}\{\vec{v}_{\sigma-1,s} + \tilde{\omega}_{\sigma-1,s}\vec{r}_{\sigma,\sigma-1}\} + \dot{\lambda}_{\sigma,\sigma-1}\vec{u}_3,$$
$$\vec{\omega}_{\sigma s} = a_{\sigma,\sigma-1}\vec{\omega}_{\sigma-1,s} + \dot{\varphi}_{\sigma,\sigma-1}\vec{u}_3. \tag{9}$$

The kinematical *conditions of connectivity* shall be given through constraint relations written in a forward computation between relative velocities of each independent closed-loop of the mechanism. Starting from the base T_0 and going to moving platform T_n, the absolute velocities $\vec{v}^A_{n0}$ and $\vec{\omega}^A_{n0}$ are computed along first leg A, for example. These vectors coincide both with the two velocities, $\vec{v}^B_{n0}$ and $\vec{\omega}^B_{n0}$, of the same platform, but computed into direction of the second leg, B. The following system of equations is obtained:

$$\vec{u}_i^T a^T_{n0}\vec{\omega}^A_{n0} = \vec{u}_i^T b^T_{n0}\vec{\omega}^B_{n0} = \vec{u}_i^T\vec{\omega}^0_n \quad (i = 1, 2, 3),$$
$$\vec{u}_i^T a^T_{n0}\{\vec{v}^A_{n0} + \tilde{\omega}^A_{n0}\vec{r}^{GA}_n\} = \vec{u}_i^T b^T_{n0}\{\vec{v}^B_{n0} + \tilde{\omega}^B_{n0}\vec{r}^{GB}_n\} = \vec{u}_i^T\dot{\vec{r}}^G_0, \tag{10}$$

where $\vec{u}_1, \vec{u}_2$ and $\vec{u}_3$ are three orthogonal unit vectors pointing, respectively, along the x_0-, y_0- and z_0-axes. The characteristic relative velocities and the conventional Jacobian are immediately obtained. This square invertible matrix is an essential element in analysis of singularities loci existing in the robot workspace.

Performing the derivatives with respect to time upon (9), we obtain the recursive form of accelerations $\vec{\gamma}_{\sigma s}$ and $\vec{\varepsilon}_{\sigma s}$:

$$\begin{aligned}\vec{\gamma}_{\sigma s} &= a_{\sigma,\sigma-1}\{\vec{\gamma}_{\sigma-1,s} + (\tilde{\omega}^2_{\sigma-1,s} + \tilde{\varepsilon}_{\sigma-1,s})\vec{r}_{\sigma,\sigma-1}\} \\ &\quad + \ddot{\lambda}_{\sigma,\sigma-1}\vec{u}_3 + 2\dot{\lambda}_{\sigma,\sigma-1}a_{\sigma,\sigma-1} \\ &\quad \times \tilde{\omega}_{\sigma-1,s}a^T_{\sigma,\sigma-1}\vec{u}_3, \\ \vec{\varepsilon}_{\sigma s} &= a_{\sigma,\sigma-1}\vec{\varepsilon}_{\sigma-1,s} + \ddot{\varphi}_{\sigma,\sigma-1}\vec{u}_3 \\ &\quad + \dot{\varphi}_{\sigma,\sigma-1}a_{\sigma,\sigma-1}\tilde{\omega}_{\sigma-1,s}a^T_{\sigma,\sigma-1}\vec{u}_3\end{aligned} \tag{11}$$

and two useful square characteristic matrices [12, 24]:

$$\begin{aligned}\tilde{\omega}_{\sigma s} &= a_{\sigma,\sigma-1}\tilde{\omega}_{\sigma-1,s}a^T_{\sigma,\sigma-1} + \dot{\varphi}_{\sigma,\sigma-1}\tilde{u}_3, \\ \tilde{\omega}^2_{\sigma s} + \tilde{\varepsilon}_{\sigma s} &= a_{\sigma,\sigma-1}\{\tilde{\omega}^2_{\sigma-1,s} + \tilde{\varepsilon}_{\sigma-1,s}\}a^T_{\sigma,\sigma-1} \\ &\quad + \dot{\varphi}^2_{\sigma,\sigma-1}\tilde{u}_3\tilde{u}_3 + \ddot{\varphi}_{\sigma,\sigma-1}\tilde{u}_3 \\ &\quad + 2\dot{\varphi}_{\sigma,\sigma-1}a_{\sigma,\sigma-1}\tilde{\omega}_{\sigma-1,s}a^T_{\sigma,\sigma-1}\tilde{u}_3.\end{aligned} \tag{12}$$

The conditions of connectivity with accelerations are

$$\vec{u}_i^T a^T_{n0}\vec{\varepsilon}^A_{n0} = \vec{u}_i^T b^T_{n0}\vec{\varepsilon}^B_{n0} = \vec{u}_i^T\vec{\varepsilon}^0_n$$
$$\vec{u}_i^T a^T_{n0}\{\vec{\gamma}^A_{n0} + (\tilde{\omega}^A_{n0}\tilde{\omega}^A_{n0} + \tilde{\varepsilon}^A_{n0})\vec{r}^{GA}_n\} \tag{13}$$
$$= \vec{u}_i^T b^T_{n0}\{\vec{\gamma}^B_{n0} + (\tilde{\omega}^B_{n0}\tilde{\omega}^B_{n0} + \tilde{\varepsilon}^B_{n0})\vec{r}^{GB}_n\} = \vec{u}_i^T\ddot{\vec{r}}^G_0.$$

These formulas give all relative linear and angular accelerations of the robot. Equations (10) and (13) constitute the *matrix kinematics model* of the constrained robotic system.

4 Equations of motion

The dynamic analysis of parallel robots is complicated by existence of a spatial kinematical structure, which possesses a large number of passive degrees of freedom, dominance of the inertial forces, frictional and gravitational components, and by the problem that is linked to real-time control in the inverse dynamics.

Three different methods lead to the same results. The first one is the Newton–Euler approach, which consists in applying the free-body diagram procedure for each body where all joint forces and moments are unknown [16, 17, 25]. Writing Newton–Euler equations once for each body of the mechanism, results

in a large system of equations that must be solved simultaneously for all the forces of constraints between two adjacent links. The second method is based on the Lagrange formalism, which introduces scalar multipliers for each kinematical closure equation [20, 27]. Because of the numerous constraints imposed by all closed-loops of parallel robot, deriving explicit equations of motion in terms of a set of independent generalized coordinates becomes a prohibitive task. The third method for the dynamic analysis, which shall be applied in the present paper, is based on the principle of virtual powers (see [28–31]). Finally, we obtain the *explicit dynamics equations of parallel robots*.

Consider the link T_τ of the mechanism connected to other two neighboring bodies by two types of joints: a prismatic joint or a revolute joint. The displacement of T_τ with respect to the last link $T_{\tau-1}$ is described by two variables: translation coordinate $\lambda_{\tau,\tau-1}$ and joint angle of rotation $\varphi_{\tau,\tau-1}$. In the first case, the rigid body T_τ moves in relative translation along the z_τ-axis under the action of the force $\vec{f}_{\tau,\tau-1} = f_{\tau,\tau-1}\vec{u}_3$ that is applied by a hydraulic or pneumatic system located in the neighboring frame $T_{\tau-1}$. In the second case, it rotates by an electric motor developing a torque of moment $\vec{m}_{\tau,\tau-1} = m_{\tau,\tau-1}\vec{u}_3$, pointed about the positive z_τ-axis. We note that for a parallel robot, a single actuator that exerts a force or a torque between two adjacent links, drives each limb.

Applying the free-body diagram procedure, Fig. 1 depicts the forces and moments acting on a typical link T_τ that is connected to link $T_{\tau-1}$ by joint O_τ and to other link $T_{\tau+1}$ by joint $O_{\tau+1}$. The forces acting on link T_τ by $T_{\tau-1}$ can be reduced about O_τ to a force $\vec{f}'_{\tau,\tau-1}$ and a moment $\vec{m}'_{\tau,\tau-1}$. Similarly, the forces acting on link T_τ by $T_{\tau+1}$ are reduced about $O_{\tau+1}$ to a resultant force $(-a^T_{\tau+1,\tau}\vec{f}'_{\tau+1,\tau})$ and a resultant moment $(-a^T_{\tau+1,\tau}\vec{m}'_{\tau+1,\tau})$, both converted into T_τ frame. Note that the vectors $\vec{f}_{n,n-1}$ and $\vec{m}_{n,n-1}$ represent the force and the moment exerted on the platform T_n by the link T_{n-1}, for $\tau = n$. When a robot carries an object, the weight of the object becomes a known load to the end-effector. Assuming that frictional force at the joints is negligible, two vectors, $\vec{f}^*_\tau$ and $\vec{m}^*_\tau$, of the wrench about the point O_τ express the action of external and internal forces, including the weight $m_\tau a_{\tau 0}\vec{g}$ of rigid body T_τ.

Now, we compute the inertia force and the resultant moment of inertia forces exerted at the joint O_τ:

$$\begin{aligned}\vec{f}^{\,\text{in}}_\tau &= -m_\tau\{\vec{\gamma}_{\tau 0} + (\tilde{\omega}^2_{\tau 0} + \tilde{\varepsilon}_{\tau 0})\vec{r}^{\,C}_\tau\},\\ \vec{m}^{\,\text{in}}_\tau &= -m_\tau\tilde{r}^{\,C}_\tau\vec{\gamma}_{\tau 0} - \hat{J}_\tau\bar{\varepsilon}_{\tau 0} - \tilde{\omega}_{\tau 0}\hat{J}_\tau\vec{\omega}_{\tau 0},\end{aligned} \tag{14}$$

where m_τ is the mass of link T_τ. Introducing a 3×3 skew-symmetric matrix $\tilde{r}_i$ *associated* with the vector $\vec{r}_i$

$$\tilde{r}_i = \begin{bmatrix} 0 & -z_i & y_i \\ z_i & 0 & -x_i \\ -y_i & x_i & 0 \end{bmatrix}, \qquad \vec{r}_i = \begin{bmatrix} x_i \\ y_i \\ z_i \end{bmatrix}, \tag{15}$$

we can express the symmetrical tensor of inertia $\hat{J}_\tau = \sum m_i\tilde{r}_i\tilde{r}_i^T$ of link T_τ, defined in a matrix form in [22].

Knowing the kinematics state of each link and the external forces acting on the robot, this paper derives the final form of explicit dynamics equations of a constrained robotic system, using the principle of virtual powers. Finally, the actuator forces and torques, required in a given motion of the end-effector, will be computed using a recursive procedure.

The parallel robot can artificially be transformed into a set of open chains, subject to the constraints. This is possible by cutting each joint for a moving platform, and it takes into account the effect by introducing the corresponding constraint conditions. The first and more complicated open tree system includes the acting link and ends with the moving platform.

The virtual displacements should be compatible with the virtual motion imposed by all kinematical constraints and joints at a given instant of time. Considering several independent virtual motions of the robot, which are compatible with the constraints, connectivity equation (10) will generate expressions of virtual velocities. By intermediate of the Jacobian matrix, absolute virtual velocities $\vec{v}^{\,v}_{\tau 0}, \vec{\omega}^{\,v}_{\tau 0}$, associated with all moving links, are related to relative virtual velocities associated with the actuated joints $\vec{v}^{\,v}_{q,q-1} = v^v_{q,q-1}\vec{u}_3$ and $\vec{\omega}^{\,v}_{q,q-1} = \omega^v_{q,q-1}\vec{u}_3$.

The principle of virtual powers states that a robot is under dynamic equilibrium if and only if the virtual powers developed by all external, internal and inertia forces vanish during any general virtual displacement, which is compatible with the kinematical constraints.

Assuming that frictional forces at the joints are negligible, the virtual power produced by the forces of constraint at the joints is zero. So, the virtual powers

contributed by the active force $\vec{f}_{q,q-1}$ and the actuator torque $\vec{m}_{q,q-1}$, the known external forces and the moments $\vec{f}_\tau^*$ and $\vec{m}_\tau^*$, and by the inertia forces and the moments of inertia forces $\vec{f}_\tau^{\,\text{in}}$ and $\vec{m}_\tau^{\,\text{in}}$, can be written as follows:

$$\vec{v}_{q,q-1}^{\,vT}\vec{f}_{q,q-1}+\vec{\omega}_{q,q-1}^{\,vT}\vec{m}_{q,q-1}+\sum_{p=1}^{l}\sum_{\tau=1}^{n_p}\left\{\vec{v}_{\tau 0}^{\,vT}\left(\vec{f}_\tau^*+\vec{f}_\tau^{\,\text{in}}\right)+\vec{\omega}_{\tau 0}^{\,vT}\left(\vec{m}_\tau^*+\vec{m}_\tau^{\,\text{in}}\right)\right\}=0, \tag{16}$$

where l denotes the number of serial independent legs fictitiously separated beginning from the fixed base and ending at the moving platform. We isolate the virtual powers developed by the active force $\vec{f}_{q,q-1}$ or the actuator torque $\vec{m}_{q,q-1}$ from these of the other known forces and inertia forces applied to all legs of the robot.

Absolute virtual velocities $\vec{v}_{\tau 0}^{\,v}$ and $\vec{\omega}_{\tau 0}^{\,v}$ can be related to the virtual relative velocities $\vec{v}_{k,k-1}^{\,v}$ and $\vec{\omega}_{k,k-1}^{\,v}$:

$$\begin{aligned}\vec{v}_{\tau 0}^{\,v}&=\sum_{k=1}^{\tau}v_{k,k-1}^{v}a_{\tau k}\vec{u}_3+\sum_{k=1}^{\tau-1}\omega_{k,k-1}^{v}a_{\tau k}\tilde{r}_{\tau k}^{T}\vec{u}_3,\\ \vec{\omega}_{\tau 0}^{\,v}&=\sum_{k=1}^{\tau}\omega_{k,k-1}^{v}a_{\tau k}\vec{u}_3,\qquad \tilde{r}_{\sigma\tau}=\sum_{\upsilon=\tau}^{\sigma-1}a_{\upsilon\tau}^{T}\tilde{r}_{\upsilon+1,\upsilon}a_{\upsilon\tau}.\end{aligned} \tag{17}$$

Introducing the following notations,

$$\begin{aligned}\vec{f}_\tau&=\sum_{\sigma=\tau}^{n}a_{\sigma\tau}^{T}\vec{f}_\sigma^{\,0},\\ \vec{m}_\tau&=\sum_{\sigma=\tau}^{n}a_{\sigma\tau}^{T}\left\{\vec{m}_\sigma^{\,0}+\sum_{\upsilon=\tau}^{\sigma-1}a_{\sigma\upsilon}\tilde{r}_{\upsilon+1,\upsilon}a_{\sigma\upsilon}^{T}\vec{f}_\sigma^{\,0}\right\},\\ \vec{f}_\sigma^{\,0}&=-\vec{f}_\sigma^{\,*}-\vec{f}_\sigma^{\,\text{in}},\qquad \vec{m}_\sigma^{\,0}=-\vec{m}_\sigma^{\,*}-\vec{m}_\sigma^{\,\text{in}},\end{aligned} \tag{18}$$

it may be observed that (16), (17) and (18) will be written in the following recursive compact form, *only* based on the relative virtual velocities $\vec{v}_{\tau,\tau-1}^{\,v}$ and $\vec{\omega}_{\tau,\tau-1}^{\,v}$:

$$v_{q,q-1}^{v}f_{q,q-1}+\omega_{q,q-1}^{v}m_{q,q-1}=\vec{u}_3^{\,T}\sum_{p=1}^{l}\sum_{\tau=1}^{n_p}\left\{v_{\tau,\tau-1}^{v}\vec{f}_\tau+\omega_{\tau,\tau-1}^{v}\vec{m}_\tau\right\}, \tag{19}$$

where

$$\begin{aligned}\vec{f}_\tau&=\vec{f}_\tau^{\,0}+a_{\tau+1,\tau}^{T}\vec{f}_{\tau+1}\\ \vec{m}_\tau&=\vec{m}_\tau^{\,0}+a_{\tau+1,\tau}^{T}\vec{m}_{\tau+1}+\tilde{r}_{\tau+1,\tau}a_{\tau+1,\tau}^{T}\vec{f}_{\tau+1}.\end{aligned} \tag{20}$$

The *dynamics model* expressed by the recursive matrix equations (19) and (20) represents the *explicit dynamics equations of a constrained robotic system* [28, 29, 33]. These equations are valid for any virtual displacement, giving the active forces $f_{q,q-1}$ or the actuator torques $m_{q,q-1}$ in terms of output forces. Using the initial values $\vec{f}_{n_p+1}=\vec{0}$ and $\vec{m}_{n_p+1}=\vec{0}$, expressions and time-history graphs of active forces and actuator torques are immediately obtained. Thus, for the force $f_{q,q-1}$ we make $v_{q,q-1}^{v}=1$ and $\omega_{q,q-1}^{v}=0$, and for the torque $m_{q,q-1}$ we consider $v_{q,q-1}^{v}=0$ and $\omega_{q,q-1}^{v}=1$. This new approach is useful for real-time control of the robots and computationally is more efficient than the Newton–Euler procedure or Lagrange formalism.

In what follows we can apply the Newton–Euler procedure to establish the set of analytical equations for each compounding rigid body of the mechanical system. These equations give all connecting forces in the external and internal joints. Several relations from the general system of equations could eventually constitute verification for the input forces or active torques obtained by the method based on the principle of virtual work. Now, we can calculate the friction forces and the friction torques in the joints, based on the friction coefficients and the maximum of the connecting forces in the joints. We apply again the explicit equations (19) and (20), where the contribution of the virtual work of friction forces in joints is added. The new active torques and input forces are compared to the values obtained in the first calculus.

The introduced method can be quickly applied in the inverse dynamics modeling of parallel robots and then the above recursive matrix equations become pure algebraic relations. But, in the direct problem of dynamics, in the same developed matrix relations there are presented many angular velocities, angular accelerations, velocities and accelerations of the mass centers, expressed as functions of the input variables of active joints and their first and second derivatives of these independent variables with respect to time.

If the input forces or the active torques are all known, the set of differential equations established for the direct dynamics simulation is numerically integrated and lead to the solutions representing the generalized coordinates of the mechanism, which determine the instantaneous position and the motion of the moving platform.

Compared with Tsai's analytical method based on the principle of virtual work [1, 13, 30], the novelties of the present approach are the following:

- Geometrical constraint relations, under matrix form, generate through successive recast the connectivity conditions that will supply all the relative velocities and relative accelerations, which characterize the independent kinematical chains.
- The accelerations of the mass centers, the angular accelerations and the twists of the inertia forces are expressed through matrix formulae, which contain the kinematical characteristics of the relative motion of the building elements of the manipulator.
- A single matrix relation supplies all the virtual velocities.
- The explicit dynamics equation represents a *definitive formula*, obtained by the transformation of the general expression of the virtual work where the relative virtual velocities only appear, generated by recursive relations.
- All intermediate analytical calculations were eliminated and the numerical computation is achieved through the numerical code, for each active force or torque applied by the driving system.

5 Advantage of the present method

Most of dynamical models based on the Lagrange formalism neglect the weight of intermediate bodies and take into consideration only the active forces or moments and the wrench of applied forces on the moving platform. The number of relations given by this approach is equal to the total number of the position variables and Lagrange multipliers inclusive. Also, the analytical calculi involved in these equations are very tedious, thus presenting an elevated error risk.

The commonly known Newton–Euler method, which takes into account the free-body-diagrams of the mechanism, leads to a large number of equations with unknowns, among which are also the connecting forces in the joints. Finally, the actuating forces or torques could be obtained.

Within the inverse kinematic analysis some exact conditions of connectivity given in (10) and (13), which define in real-time the position, velocity and acceleration of each element of the parallel robot, have been established in this paper. The dynamics model takes into consideration the masses and forces of inertia introduced by all component elements of the parallel robot.

The new approach based on the principle of virtual powers can eliminate all forces of internal joints and establishes a direct determination of the time-history evolution of torques required by the actuators. The recursive matrix equations (19) and (20) represent the explicit equations of the dynamics simulation and can easily be transformed into a model for automatic command of a parallel robot.

In conclusion, the novel matrix model may successfully be applied in forward and inverse mechanics of parallel robots, the end-effectors of which participate in a translation motion or a mixed motion.

6 Two examples

6.1 Parallel cube-robot

As the first application in what follows, some recursive matrix relations for the kinematics and dynamics of a three translational DOFs parallel cube-robot are established. The concurrent actuators are arranged according to the Cartesian coordinate system with fixed orientation, which means that the actuating directions are normal to each other (Fig. 2). For this reason this type of mechanism is called a cube-robot.

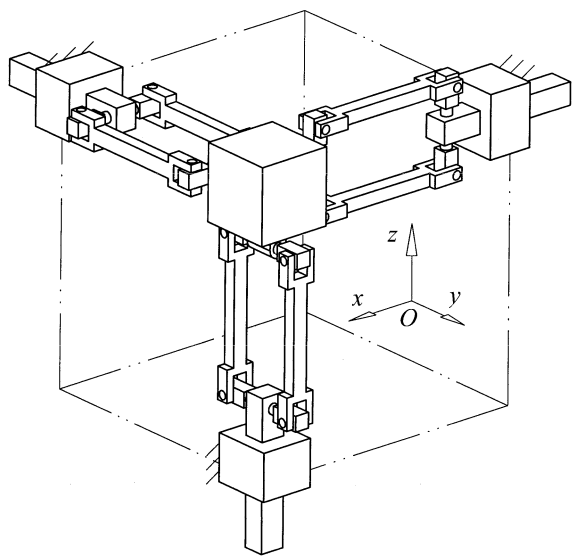

Fig. 2 The parallel cube-robot

This prototype of the robot [32] has technological advantages such as: symmetrical design, regular workspace shape properties with a bounded velocity amplification factor and low inertia effect.

6.1.1 *Inverse geometric model*

The mechanism input of the robot is made up of three actuated orthogonal prismatic joints. The output body is connected to the prismatic joints through a set of three identical kinematical chains (Fig. 3).

The architecture of one of the three parallel closed chains of the cube-robot consists of an active prismatic system, a passive revolute joint, an intermediate mechanism with four revolute links that connect four bars, which are parallel two by two, ending with a passive revolute link connected to the moving platform. Inside each chain, the parallelogram mechanism is used and oriented in a manner that the end-effector is restricted to *translation* movement only. The arrangement of the joints in the chains has been defined to eliminate any constraint singularity in the Cartesian workspace [2, 3].

Let us locate a fixed reference frame $O-x_0y_0z_0(T_0)$ (see Fig. 3) at the intersection point of three axes of actuated prismatic joints, about which the three-degrees-of-freedom robot moves. It has three legs of known dimensions and masses. To simplify the graphical image of the kinematical scheme of the mechanism, in the following we will represent the intermediate reference systems by only two axes, as is given in most of literature [1, 7, 26]. The z_k-axis is represented, of course, for each component element T_k. We mention that the relative rotation or relative translation with $\varphi_{k,k-1}$ angle or $\lambda_{k,k-1}$ displacement of T_k body must be always pointing about or along the direction of the z_k-axis.

The first element of the leg A is one of the three active *sliders* of the upside-down robot. It is a homogeneous rod of the length $A_1A_2 = l_1$ and the mass m_1, moving horizontally along the z_1^A-axis with a displacement λ_{10}^A. The center of the transmission rod $A_3A_6 = l_2$ is denoted by A_2. This link is connected to the frame $A_2-x_2^Ay_2^Az_2^A$ (called T_2^A) and it has a relative rotation about the z_2^A-axis with the angle φ_{21}^A, so that $\omega_{21}^A = \dot{\varphi}_{21}^A$ and $\varepsilon_{21}^A = \ddot{\varphi}_{21}^A$. It has the mass m_2 and the central tensor of inertia $\hat{J}_2$. Moreover, two identical and parallel bars A_3A_4 and A_6A_7 with the same length l_3 rotate about the T_2^A frame with the angle $\varphi_{32}^A = \varphi_{62}^A$. They have also the same mass m_3 and the same tensor of inertia $\hat{J}_3$. The four-bar parallelogram is closed by an element T_4^A which is identical with T_2^A. Its tensor of inertia is $\hat{J}_4$. This element rotates with the relative angle $\varphi_{43}^A = \varphi_{32}^A$.

The center A_5 of the interval between the two revolute joints connects with the moving platform $A_5-x_5^Ay_5^Az_5^A(T_5^A)$. The platform of the robot can be a cube of mass m_5, central tensor of inertia $\hat{J}_5$ and side dimension l, which rotate relatively by an angle φ_{54}^A with respect to the neighboring body T_4^A. Finally, another

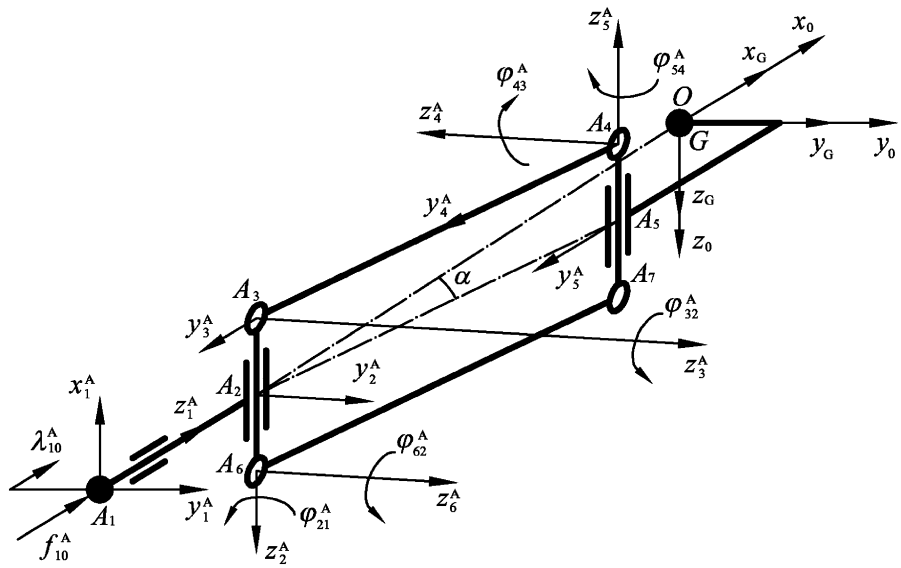

Fig. 3 Kinematical scheme of the leg A of the upside-down cube-robot

reference system $G - x_G y_G z_G$ is located at the center G of the cubic moving platform.

Due to the special arrangement of the four-bar parallelograms and the three prismatic joints at points A_1, B_1 and C_1, the mechanism has three translation degrees of freedom. This unique characteristic is useful in many applications, such as a $x - y - z$ positioning device. The angle α gives the initial orientation of the three upper arms about their guide-ways.

The three concurrent displacements, λ_{10}^A, λ_{10}^B and λ_{10}^C, of the actuators A_1, B_1 and C_1 are the input variables of active joints that give the *input vector* $\vec{\lambda}_{10}$ of the instantaneous position of the mechanism. But, the objective of the inverse geometric problem is to find the vector $\vec{\lambda}_{10}$ and the position of the robot with the given three absolute coordinates of the center G of the platform x_0^G, y_0^G and z_0^G.

Pursuing the three legs A, B and C, we obtain the following transformation matrices:

$$\begin{aligned}
&a_{10} = a_1, && a_{21} = a_{21}^{\varphi} a_\alpha a_2, && a_{32} = a_{32}^{\varphi} a_3,\\
&a_{43} = a_{32}^{\varphi} a_4, && a_{54} = a_{54}^{\varphi} a_\alpha a_2, && a_{62} = a_{32},\\
&b_{10} = a_5, && b_{21} = b_{21}^{\varphi} a_\alpha a_2, && b_{32} = b_{32}^{\varphi} a_3,\\
&b_{43} = b_{32}^{\varphi} a_4, && b_{54} = b_{54}^{\varphi} a_\alpha a_2, && b_{62} = b_{32},\\
&c_{10} = a_6, && c_{21} = c_{21}^{\varphi} a_\alpha a_2, && c_{32} = c_{32}^{\varphi} a_3,\\
&c_{43} = c_{32}^{\varphi} a_4, && c_{54} = c_{54}^{\varphi} a_\alpha a_2, && c_{62} = c_{32},
\end{aligned} \tag{21}$$

where we denote [22]

$$a_1 = \begin{bmatrix} 0 & 0 & -1 \\ 0 & 1 & 0 \\ 1 & 0 & 0 \end{bmatrix}, \qquad a_2 = \begin{bmatrix} 0 & 0 & 1 \\ 0 & 1 & 0 \\ -1 & 0 & 0 \end{bmatrix},$$

$$a_3 = \begin{bmatrix} 0 & 0 & -1 \\ -1 & 0 & 0 \\ 0 & 1 & 0 \end{bmatrix}, \qquad a_4 = \begin{bmatrix} -1 & 0 & 0 \\ 0 & 1 & 0 \\ 0 & 0 & -1 \end{bmatrix},$$

$$a_5 = \begin{bmatrix} -1 & 0 & 0 \\ 0 & 0 & 1 \\ 0 & 1 & 0 \end{bmatrix}, \qquad a_6 = \begin{bmatrix} 0 & -1 & 0 \\ 1 & 0 & 0 \\ 0 & 0 & 1 \end{bmatrix}, \tag{22}$$

$$a_\alpha = \begin{bmatrix} \cos\alpha & \sin\alpha & 0 \\ -\sin\alpha & \cos\alpha & 0 \\ 0 & 0 & 1 \end{bmatrix},$$

$$a_{k,k-1}^{\varphi} = \begin{bmatrix} \cos\varphi_{k,k-1}^A & \sin\varphi_{k,k-1}^A & 0 \\ -\sin\varphi_{k,k-1}^A & \cos\varphi_{k,k-1}^A & 0 \\ 0 & 0 & 1 \end{bmatrix},$$

$$a_{k0} = \prod_{j=1}^{k} a_{k-j+1,k-j} \quad (k = 1, 2, \ldots, 5).$$

The translation conditions for the platform are expressed by the following identities:

$$a_{50}^{\circ T} a_{50} = b_{50}^{\circ T} b_{50} = c_{50}^{\circ T} c_{50} = I, \tag{23}$$

where

$$a_{50}^{\circ} = \begin{bmatrix} 0 & -1 & 0 \\ -1 & 0 & 0 \\ 0 & 0 & -1 \end{bmatrix},$$

$$b_{50}^{\circ} = \begin{bmatrix} 0 & 0 & -1 \\ 0 & -1 & 0 \\ -1 & 0 & 0 \end{bmatrix}, \tag{24}$$

$$c_{50}^{\circ} = \begin{bmatrix} -1 & 0 & 0 \\ 0 & -1 & 0 \\ 0 & 0 & 1 \end{bmatrix}.$$

From these relations, one obtains the following relations between angles:

$$\varphi_{54}^A = \varphi_{21}^A, \qquad \varphi_{54}^B = \varphi_{21}^B, \qquad \varphi_{54}^C = \varphi_{21}^C. \tag{25}$$

For the inverse geometric analysis, the position of an end-point $P(x_0^P, y_0^P, z_0^P)$ is treated as known and the goal is to find the joint variables λ_{10}^A, λ_{10}^B and λ_{10}^C that yield the given location of the tool. If the aim is to generate a sequence of points to move the tool along an arc, care must be taken to avoid branch switching during motion, which may cause inefficient or impossible robot motions. Moreover, leg singularities may occur at which the robot loses DOF and the joint variables become linearly dependent.

Suppose, for example, that the *rectilinear motion* of the mass center G of the platform is expressed by the following relations:

$$\vec{r}_0^G = \begin{bmatrix} x_0^G & y_0^G & z_0^G \end{bmatrix},$$

$$\begin{aligned} x_0^G &= x_0^{G*}\left(1 - \cos\frac{2\pi}{3}t\right), \\ y_0^G &= y_0^{G*}\left(1 - \cos\frac{2\pi}{3}t\right), \\ z_0^G &= z_0^{G*}\left(1 - \cos\frac{2\pi}{3}t\right), \end{aligned} \tag{26}$$

the inputs $\lambda_{10}^A, \lambda_{10}^B$ and λ_{10}^C of the robots and the variables $\varphi_{21}^A, \varphi_{32}^A, \varphi_{21}^B, \varphi_{32}^B, \varphi_{21}^C, \varphi_{32}^C$ will be given by the following geometrical conditions:

$$\begin{aligned} &\vec{r}_{10}^A + \sum_{k=1}^{4} a_{k0}^T \vec{r}_{k+1,k}^A + a_{50}^T \vec{r}_5^{GA} \\ &\quad = \vec{r}_{10}^B + \sum_{k=1}^{4} b_{k0}^T \vec{r}_{k+1,k}^B + b_{50}^T \vec{r}_5^{GB} \\ &\quad = \vec{r}_{10}^C + \sum_{k=1}^{4} c_{k0}^T \vec{r}_{k+1,k}^C + c_{50}^T \vec{r}_5^{GC} = \vec{r}_0^G, \end{aligned} \tag{27}$$

where, for example, one denotes

$$\vec{u}_1 = \begin{bmatrix} 1 \\ 0 \\ 0 \end{bmatrix}, \qquad \vec{u}_2 = \begin{bmatrix} 0 \\ 1 \\ 0 \end{bmatrix}, \qquad \vec{u}_3 = \begin{bmatrix} 0 \\ 0 \\ 1 \end{bmatrix},$$

$$\tilde{u}_3 = \begin{bmatrix} 0 & -1 & 0 \\ 1 & 0 & 0 \\ 0 & 0 & 0 \end{bmatrix},$$

$$\begin{aligned} \vec{r}_{10}^A &= \left(\lambda_{10}^A - l_1 - l_3\cos\alpha - \frac{l}{2}\right) a_{10}^T \vec{u}_3, \\ \vec{r}_{21}^A &= l_1 \vec{u}_3, \qquad \vec{r}_{32}^A = -\frac{l_2}{2}\vec{u}_3, \\ \vec{r}_{43}^A &= -l_3 \vec{u}_2, \qquad \vec{r}_{54}^A = \frac{l_2}{2}\vec{u}_1, \\ \vec{r}_5^{GA} &= \begin{bmatrix} l_3\sin\alpha & -\frac{l}{2} & 0 \end{bmatrix}^T. \end{aligned} \tag{28}$$

Actually, these equations mean that there is only one inverse geometric solution for the robot:

$$\begin{aligned} &\sin\varphi_{32}^A = -\frac{z_0^G}{l_3}, \qquad \sin\left(\varphi_{21}^A + \alpha\right) = \frac{y_0^G + l_3\sin\alpha}{l_3\cos\varphi_{32}^A}, \\ &\lambda_{10}^A = x_0^G + l_3\cos\alpha - l_3\cos\left(\varphi_{21}^A + \alpha\right)\cos\varphi_{32}^A, \\ &\sin\varphi_{32}^B = -\frac{x_0^G}{l_3}, \qquad \sin\left(\varphi_{21}^B + \alpha\right) = \frac{z_0^G + l_3\sin\alpha}{l_3\cos\varphi_{32}^B}, \end{aligned} \tag{29}$$

$$\lambda_{10}^B = y_0^G + l_3\cos\alpha - l_3\cos\left(\varphi_{21}^B + \alpha\right)\cos\varphi_{32}^B,$$

$$\sin\varphi_{32}^C = -\frac{y_0^G}{l_3}, \qquad \sin\left(\varphi_{21}^C + \alpha\right) = \frac{x_0^G + l_3\sin\alpha}{l_3\cos\varphi_{32}^C},$$

$$\lambda_{10}^C = z_0^G + l_3\cos\alpha - l_3\cos\left(\varphi_{21}^C + \alpha\right)\cos\varphi_{32}^C.$$

6.1.2 Robot kinematics

We develop the inverse kinematics problem and determine the velocities and accelerations of the robot, supposing that the translation motion of the moving platform is known.

The kinematics of the component elements of each leg (for example, the leg A) are characterized by angular velocities $\vec{\omega}_{k0}^A$ and linear velocities $\vec{v}_{k0}^A$ of the joints A_k, given by (9):

$$\begin{aligned} &\vec{\omega}_{k0}^A = a_{k,k-1}\vec{\omega}_{k-1,0}^A + \omega_{k,k-1}^A \vec{u}_3, \quad \omega_{k,k-1}^A = \dot{\varphi}_{k,k-1}^A, \\ &\vec{v}_{k0}^A = a_{k,k-1}\left\{\vec{v}_{k-1,0}^A + \tilde{\omega}_{k-1,0}^A \vec{r}_{k,k-1}^A\right\}, \\ &\vec{v}_{10}^A = \dot{\lambda}_{10}^A \vec{u}_3. \end{aligned} \tag{30}$$

If the other two kinematical chains of the robot are pursued, analogous relations can be easily obtained.

Equations (23) and (27) of geometric constraints can be differentiated with respect to time to obtain the following *matrix conditions of connectivity* [23]:

$$\begin{aligned} &\omega_{21}^A \vec{u}_i^T a_{20}^T \vec{u}_3 + \omega_{54}^A \vec{u}_i^T a_{50}^T \vec{u}_3 = 0, \\ &v_{10}^A \vec{u}_i^T a_{10}^T \vec{u}_3 + l_3\omega_{21}^A \vec{u}_i^T a_{20}^T \tilde{u}_3 a_{32}^T \vec{u}_2 \\ &\quad + l_3\omega_{32}^A \vec{u}_i^T a_{30}^T \tilde{u}_3 \vec{u}_2 = \vec{u}_i^T \dot{\vec{r}}_0^G \quad (i = 1, 2, 3), \end{aligned} \tag{31}$$

where $\tilde{u}_1, \tilde{u}_2, \tilde{u}_3$ are skew-symmetric matrices associated to the three orthogonal unit vectors $\vec{u}_1, \vec{u}_2, \vec{u}_3$. From these equations, relative velocities $v_{10}^A, \omega_{21}^A, \omega_{32}^A$ and $\omega_{54}^A = \omega_{21}^A$ result as functions of the translation velocity of the platform. Equation (31) gives the *complete* Jacobian matrix of the robot. This matrix is a fundamental element for the analysis of the robot workspace and the particular configurations of singularities where the robot becomes uncontrollable.

Rearranging, the above nine equations in (29) of the cube-robot can be immediately written as follows:

$$\left(x_0^G + l_3\cos\alpha - \lambda_{10}^A\right)^2 + \left(y_0^G + l_3\sin\alpha\right)^2 + z_0^{G2} = l_3^2,$$

$$\left(y_0^G + l_3\cos\alpha - \lambda_{10}^B\right)^2 + \left(z_0^G + l_3\sin\alpha\right)^2 + x_0^{G2} = l_3^2,$$
$$\left(z_0^G + l_3\cos\alpha - \lambda_{10}^C\right)^2 + \left(x_0^G + l_3\sin\alpha\right)^2 + y_0^{G2} = l_3^2, \tag{32}$$

where the "zero" position $\vec{r}_0^{0G} = [0\ 0\ 0]^T$ corresponds to the joints' variables $\vec{\lambda}_{10}^0 = [0\ 0\ 0]^T$. The derivative of conditions (32) with respect to time leads to the matrix equation

$$J_1\dot{\vec{\lambda}}_{10} = J_2\dot{\vec{r}}_0^G. \tag{33}$$

Matrices J_1 and J_2 are, respectively, the inverse and forward Jacobian of the robot and can be expressed as

$$J_1 = \operatorname{diag}\{\alpha_1 \quad \alpha_2 \quad \alpha_3\},$$
$$J_2 = \begin{bmatrix} \alpha_1 & \beta_2 & z_0^G \\ x_0^G & \alpha_2 & \beta_3 \\ \beta_1 & y_0^G & \alpha_3 \end{bmatrix}, \tag{34}$$

with

$$\begin{aligned} \alpha_1 &= x_0^G + l_3\cos\alpha - \lambda_{10}^A, \\ \alpha_2 &= y_0^G + l_3\cos\alpha - \lambda_{10}^B, \\ \alpha_3 &= z_0^G + l_3\cos\alpha - \lambda_{10}^C, \\ \beta_1 &= x_0^G + l_3\sin\alpha, \\ \beta_2 &= y_0^G + l_3\sin\alpha, \\ \beta_3 &= z_0^G + l_3\sin\alpha. \end{aligned} \tag{35}$$

We assume a virtual motion of the robot with the generalized velocities $v_{10a}^{Av} = 1$, $v_{10a}^{Bv} = 0$, $v_{10a}^{Cv} = 0$.

The characteristic virtual velocities are expressed as functions of the position of the mechanism by the kinematical constraint equations of two independent loops, $A - B$ and $B - C$:

$$\vec{u}_i^T a_{50}^T \vec{v}_{50a}^{Av} = \vec{u}_i^T b_{50}^T \vec{v}_{50a}^{Bv} = \vec{u}_i^T c_{50}^T \vec{v}_{50a}^{Cv} \quad (i = 1, 2, 3),$$
$$\omega_{54a}^{Av} = \omega_{21a}^{Av}, \qquad \omega_{54a}^{Bv} = \omega_{21a}^{Bv}, \qquad \omega_{54a}^{Cv} = \omega_{21a}^{Cv}. \tag{36}$$

Some other relations of connectivity can be obtained if one considers successively that $v_{10b}^{Bv} = 1$, $v_{10b}^{Cv} = 0$, $v_{10b}^{Av} = 0$, $v_{10c}^{Cv} = 1$, $v_{10c}^{Av} = 0$, and $v_{10c}^{Bv} = 0$.

As for the relative accelerations $\gamma_{10}^A, \varepsilon_{21}^A, \varepsilon_{32}^A$ and $\varepsilon_{54}^A = \varepsilon_{21}^A$ of the robot, the derivatives of (31) give the other following conditions of connectivity:

$$\begin{aligned} &\varepsilon_{21}^A \vec{u}_i^T a_{20}^T \vec{u}_3 + \varepsilon_{54}^A \vec{u}_i^T a_{50}^T \vec{u}_3 = 0, \\ &\gamma_{10}^A \vec{u}_i^T a_{10}^T \vec{u}_3 + l_3\varepsilon_{21}^A \vec{u}_i^T a_{20}^T \tilde{u}_3 a_{32}^T \vec{u}_2 + l_3\varepsilon_{32}^A \vec{u}_i^T a_{30}^T \tilde{u}_3 \vec{u}_2 \\ &\quad = \vec{u}_i^T \ddot{\vec{r}}_0^G - l_3\omega_{21}^A\omega_{21}^A \vec{u}_i^T a_{20}^T \tilde{u}_3\tilde{u}_3 a_{32}^T \vec{u}_2 \\ &\quad\quad - l_3\omega_{32}^A\omega_{32}^A \vec{u}_i^T a_{30}^T \tilde{u}_3\tilde{u}_3\vec{u}_2 \\ &\quad\quad - 2l_3\omega_{21}^A\omega_{32}^A \vec{u}_i^T a_{20}^T \tilde{u}_3 a_{32}^T \tilde{u}_3\vec{u}_2 \quad (i = 1, 2, 3) \end{aligned} \tag{37}$$

The angular accelerations $\vec{\varepsilon}_{k0}^A$ and the accelerations $\vec{\gamma}_{k0}^A$ of joints A_k are easily calculated by (11). Equations (31) and (37) represent the *inverse kinematics model* of the parallel cube-robot.

6.1.3 Inverse robot dynamics

In the context of the real-time control, neglecting the friction forces and considering the gravitational effects, the relevant objective of the dynamics is to determine the input forces, which must be exerted by the actuators in order to produce a given trajectory of the effector.

Three independent mechanical systems, A_1, B_1, and C_1, that generate three spatial forces, $\vec{f}_{10}^A = f_{10}^A\vec{u}_3$, $\vec{f}_{10}^B = f_{10}^B\vec{u}_3$, and $\vec{f}_{10}^C = f_{10}^C\vec{u}_3$, which are concurrent in O and oriented along the z_1^A-, z_1^B-, and z_1^C-axes, control the motion of the three sliders of the robot.

The force of inertia and the resultant moment of the forces of inertia of an arbitrary rigid body T_k are determined with respect to the joint's center A_k. On the other hand, the wrench of two vectors, $\vec{f}_k^*$ and $\vec{m}_k^*$, evaluates the influence of the action of the weight $m_k\vec{g}$ and the influence of other external and internal forces applied to the same element T_k of the robot.

Knowing the position and kinematics state of each link, as well as the external forces acting on the robot, in what follows one applies the principle of virtual powers for an inverse dynamic problem.

The active forces required in a given motion of the moving platform will be determined in the inverse dynamic problem by using of the fundamental equations (19) and (20) of parallel robot dynamics.

Thus, the force f_{10}^A of the first actuator A_1 is expressed by a compact matrix formula

$$
\begin{aligned}
f_{10}^{A} = \vec{u}_3^{T}\big[&\vec{F}_1^{A} + .\omega_{54a}^{Av}\vec{M}_5^{A} \\
&+ \omega_{21a}^{Av}\vec{M}_2^{A} + \omega_{32a}^{Av}\big(\vec{M}_3^{A} + \vec{M}_4^{A} + \vec{M}_6^{A}\big) \\
&+ \omega_{21a}^{Bv}\vec{M}_2^{B} + \omega_{32a}^{Bv}\big(\vec{M}_3^{B} + \vec{M}_4^{B} + \vec{M}_6^{B}\big) \\
&+ \omega_{21a}^{Cv}\vec{M}_2^{C} + \omega_{32a}^{Cv}\big(\vec{M}_3^{C} + \vec{M}_4^{C} + \vec{M}_6^{C}\big)\big], \quad (38)
\end{aligned}
$$

where, for example, one denotes:

$$
\begin{aligned}
&\vec{F}_{k0}^{A} = m_k^{A}\big[\vec{\gamma}_{k0}^{A} + \big(\tilde{\omega}_{k0}^{A}\tilde{\omega}_{k0}^{A} + \tilde{\varepsilon}_{k0}^{A}\big)\vec{r}_k^{CA}\big] - \vec{f}_k^{*A}, \\
&\vec{M}_{k0}^{A} = m_k^{A}\tilde{r}_k^{CA}\vec{\gamma}_{k0}^{A} + \hat{J}_k^{A}\vec{\varepsilon}_{k0}^{A} + \tilde{\omega}_{k0}^{A}\hat{J}_k^{A}\vec{\omega}_{k0}^{A} - \vec{m}_k^{*A}, \\
&\vec{F}_k^{A} = \vec{F}_{k0}^{A} + a_{k+1,k}^{T}\vec{F}_{k+1} \quad (k = 6, 5, \ldots, 1), \quad (39) \\
&\vec{M}_k^{A} = \vec{M}_{k0}^{A} + a_{k+1,k}^{T}\vec{M}_{k+1} + \tilde{r}_{k+1,k}^{T}a_{k+1,k}^{T}\vec{F}_{k+1}, \\
&\vec{f}_k^{*A} = 9.81 m_k^{A} a_{k0}\vec{u}_3, \qquad \vec{m}_k^{*A} = 9.81 m_k^{A}\tilde{r}_k^{CA}a_{k0}\vec{u}_3.
\end{aligned}
$$

Equations (38) and (39) represent the *inverse dynamics model* of the parallel cube-robot.

As application let us consider a robot which has the following characteristics:

$$
\begin{aligned}
&x_0^{G*} = 0.10 \text{ m}, \qquad y_0^{G*} = 0.05 \text{ m}, \\
&z_0^{G*} = -0.15 \text{ m}, \\
&l = 0.20 \text{ m}, \qquad l_1 = 0.15 \text{ m}, \\
&l_2 = 0.08 \text{ m}, \qquad l_3 = 0.85 \text{ m}, \\
&l_4 = l_2, \qquad \alpha = \frac{\pi}{36}, \qquad \Delta t = 3 \text{ s}, \\
&m_1 = 0.35 \text{ kg}, \qquad m_2 = 0.2 \text{ kg}, \qquad m_3 = 2.5 \text{ kg}, \\
&m_4 = m_2, \qquad m_5 = 15 \text{ kg}, \qquad m_6 = m_3.
\end{aligned}
$$

Depending of masses and inertias of all links, numerically we obtain, for example, the time evolution of forces f_{10}^{A} (Fig. 4), f_{10}^{B} (Fig. 5) and f_{10}^{C} (Fig. 6) of three prismatic actuators.

6.2 A new space parallel robot

The mechanism input of the second case study is made up of three actuated prismatic joints, while the output body is connected to the fixed base through a set of three legs (see Fig. 7). The first and second legs have identical kinematical chains, which are two prismatic-revolute-universal (*PRU*) chains. Being very different from the two legs, the third leg is a prismatic-revolute-cylindrical (*PRC*) chain. The robot has two translation degrees of freedom and one rotation degree of freedom.

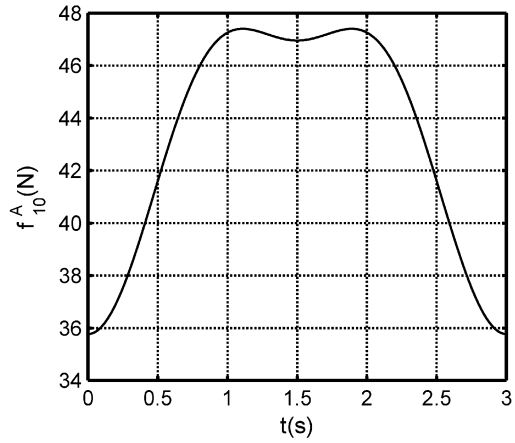

Fig. 4 Force f_{10}^{A} of the first actuator

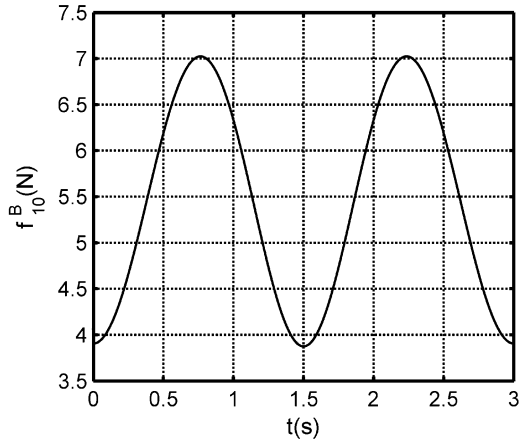

Fig. 5 Force f_{10}^{B} of the second actuator

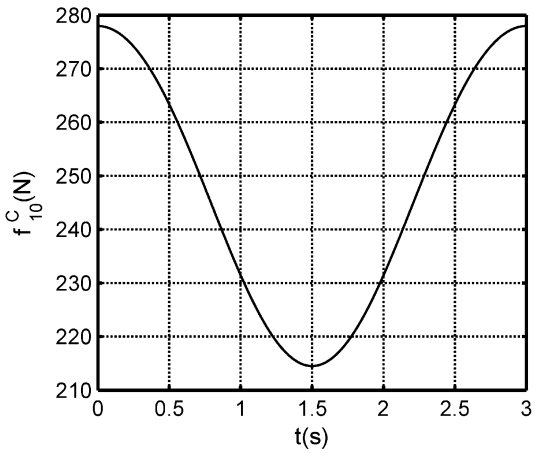

Fig. 6 Force f_{10}^{C} of the third actuator

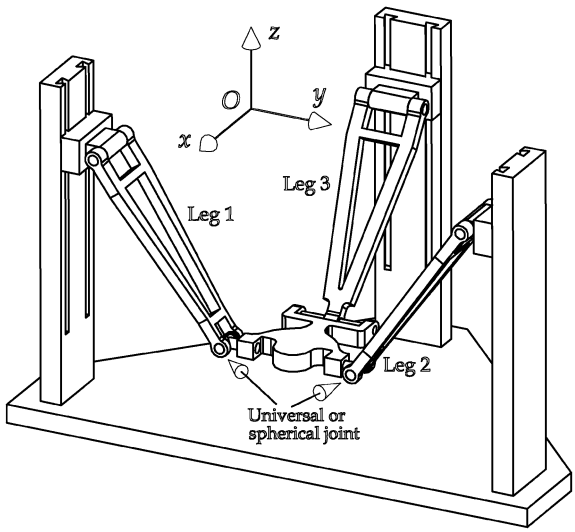

Fig. 7 A new space parallel robot

In this section, the above recursive matrix method is adopted to derive the kinematics model and the inverse dynamics equations of this spatial parallel robot.

6.2.1 Geometric model

The motion of the platform is accomplished by three sliders along the guide-ways. The mechanism contains a moving platform $A_3B_3C_4$ of mass m_4 and the tensor of inertia $\hat{J}_4$, which is an isosceles triangle described by the sizes $PC_4 = L_1$ and $PA_3 = PB_3 = r$ (Fig. 8). The vertices of this platform are connected through three legs to the sliders of a fixed base $A_0B_0C_0 = A_1B_1C_1$, which is also an isosceles triangles described by the sizes $O_0A_1 = O_0B_1 = R$ and $O_0C_1 = L_3$.

Each of three limbs consists of a lower link and an upper arm. The lower links A_1A_2 and B_1B_2 of two identical legs are connected to the fixed base through active revolute joints A_1 and B_1 and to the upper arms with passive revolute joints A_2 and B_2. These lower links have also the same mass m_1. The two identical upper arms, having the lengths $A_2A_3 = R_2$ and $B_2B_3 = R_2$, the same mass m_2 and the same tensor of inertia $\hat{J}_2$, are then connected to the moving platform by two universal or spherical joints, A_3 and B_3. The third leg consists of an active prismatic system, a revolute joint C_2 that is attached to the third slider C_1C_2 of mass m_1, an intermediary rod of length $C_2C_3 = L_2$, mass m_2 and tensor of inertia $\hat{J}_2$, which is connected to the moving platform by a cylindrical joint C_3.

The motion of the moving platform $A_3B_3C_4$ can be accomplished with three input linear displacements, λ_{10}^A, λ_{10}^B and λ_{10}^C, which are given by the three prismatic actuators, A_1, B_1 and C_1. A fixed global frame $O_0 - x_0y_0z_0$ is located at the center of the side A_1B_1, with the z_0-axis normal to the base platform and the y_0-axis is pointing along A_1B_1. The 3-DOF robot is moving with respect to this Cartesian reference. Another reference frame, $P - x_Py_Pz_P$, called the top frame, is located at the center of the side A_3B_3. The z_P-axis is perpendicular to the output platform and the y_P-axis is directed along A_3B_3.

One of the three active elements of the robot is the first body C_1C_2 of the third upside-down limb C (leg 3), for example. Mounted on the guide-way, this slider effects a vertical translation with the displacement λ_{10}^C. A local leg frame $C_2 - x_2^C y_2^C z_2^C$ is attached to a transmission rod with its origin at point C_2, the z_2^C direction along the horizontal rotating axis of the revolute joint. This upper arm has a relative rotation about the z_2^C-axis with the angle φ_{21}^C, angular velocity $\omega_{21}^C = \dot{\varphi}_{21}^C$ and angular acceleration $\varepsilon_{21}^C = \ddot{\varphi}_{21}^C$.

Further on, a fictitious frame $C_3 - x_3^C y_3^C z_3^C$ has a relative translation along the horizontal z_3^C-axis with the displacement λ_{32}^C so that $v_{32}^C = \dot{\lambda}_{32}^C$ and $\gamma_{32}^C = \ddot{\lambda}_{32}^C$.

Finally, a passive revolute joint C_4 connects the moving platform $A_3B_3C_4$ to the frame $C_4 - x_4y_4z_4(T_4)$, which rotates relatively about the z_4^C-axis by the angle φ_{43}^C and angular velocity $\omega_{43}^C = \dot{\varphi}_{43}^C$.

Due to the arrangement of the links and joints, the axes of the passive revolute joints in the first and second legs are parallel to each other. In such a way, the two legs can provide two constraints on the moving platform with the rotation about the z_0-axis and the translation along the x_0-axis. The third leg can provide two constraints on the rotation of moving platform about z_0 and x_0 axes. This leaves the mechanism with two translation degrees of freedom in $O_0 - y_0z_0$ plane and one rotation degree of freedom about the y_0-axis.

The displacements λ_{10}^A, λ_{10}^B and λ_{10}^C of the three actuators, A_1, B_1 and C_1, are considered as parameters, which give the input vector $\vec{\lambda}_{10} = [\lambda_{10}^A \ \lambda_{10}^B \ \lambda_{10}^C]^T$ of the instantaneous position of the robot. But, in the inverse geometric problem, one can suppose that the coordinates y_0^P and z_0^P of the point P and the rotational angle ϕ of the platform give the position of the mechanism. Starting from the origin of the reference O_0 and pursuing the three serial chains, $A_1A_2A_3$, $B_1B_2B_3$ and

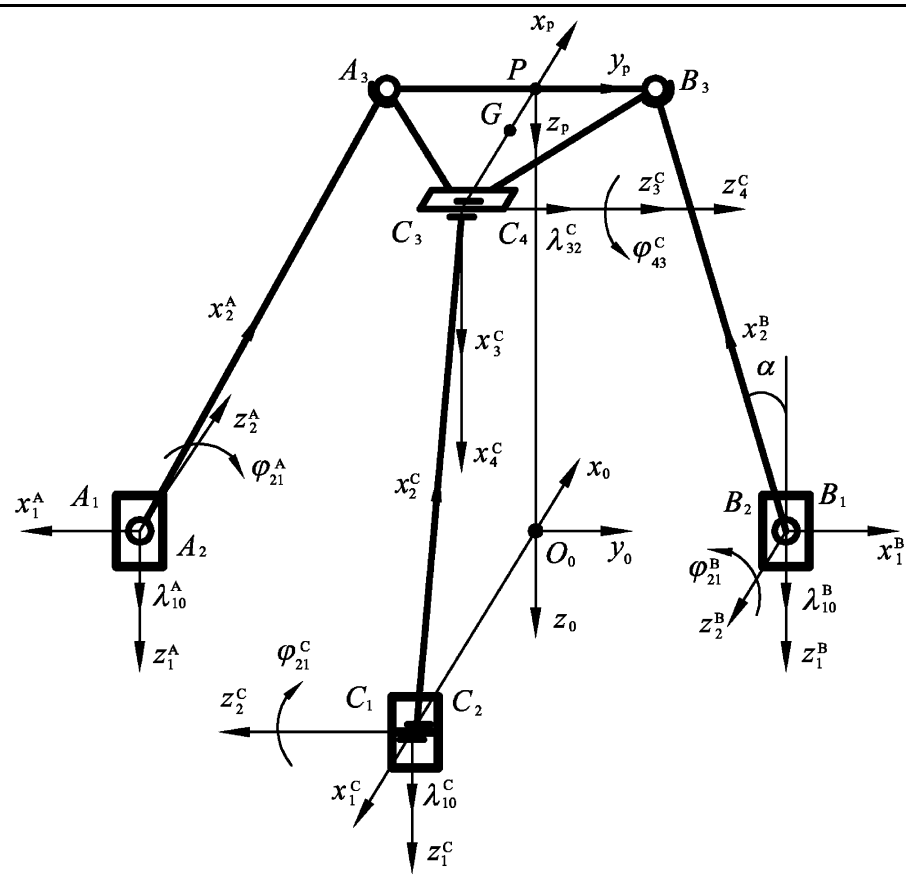

Fig. 8 Kinematical scheme of the upside-down mechanism

$C_1C_2C_3C_4$, we obtains the following transformation matrices:

$$\begin{aligned} a_{10} &= \theta_2^T, \qquad a_{21} = a_{21}^{\varphi} a_\alpha \theta_1 \theta_2, \\ b_{10} &= \theta_2, \qquad b_{21} = b_{21}^{\varphi} a_\alpha \theta_1 \theta_2, \\ c_{10} &= \theta_4, \qquad c_{21} = c_{21}^{\varphi} a_\alpha \theta_1 \theta_2, \\ c_{32} &= a_\alpha \theta_3, \qquad c_{43} = c_{43}^{\varphi}, \end{aligned} \tag{40}$$

where, for example,

$$\theta_1 = \begin{bmatrix} 0 & 0 & -1 \\ 0 & 1 & 0 \\ 1 & 0 & 0 \end{bmatrix}, \qquad \theta_2 = \begin{bmatrix} 0 & 1 & 0 \\ -1 & 0 & 0 \\ 0 & 0 & 1 \end{bmatrix},$$

$$\theta_3 = \begin{bmatrix} -1 & 0 & 0 \\ 0 & 1 & 0 \\ 0 & 0 & -1 \end{bmatrix}, \qquad \theta_4 = \begin{bmatrix} -1 & 0 & 0 \\ 0 & -1 & 0 \\ 0 & 0 & 1 \end{bmatrix}. \tag{41}$$

Rotation condition concerning the absolute orientation of the moving platform is given by the following identity:

$$c_{40}^{\circ T} c_{40} = a \tag{42}$$

and by the matrices

$$\mathbf{c}_{40}^{\circ} = \begin{bmatrix} 0 & 0 & 1 \\ 1 & 0 & 0 \\ 0 & 1 & 0 \end{bmatrix}, \qquad a = R^T = \begin{bmatrix} \cos\phi & 0 & -\sin\phi \\ 0 & 1 & 0 \\ \sin\phi & 0 & \cos\phi \end{bmatrix}, \tag{43}$$

where a is the rotation matrix about the y_P-axis and the resulting matrix $c_{40} = c_{43}c_{32}c_{21}c_{10}$ is obtained by multiplying five basic matrices. From this relation, one

obtains the first relation between the angles of rotation: $\phi = \varphi_{43}^C - \varphi_{21}^C$ with

$$\phi = \phi_0^* \left[1 - \cos\left(\frac{\pi}{3} t \right) \right]. \tag{44}$$

Consider, for example, that the platform moves for six seconds and the motion of the characteristic point P along *vertical ellipses* is expressed by the following functions:

$$\begin{aligned} \vec{\mathbf{r}}_0^P &= [0 \quad y_0^P \quad z_0^P]^T, \\ y_0^P &= y_0^{P*} \sin\left(\frac{\pi}{3} t \right), \\ z_0^P &= -h + z_0^{P*} \left[1 - \cos\left(\frac{\pi}{3} t \right) \right]. \end{aligned} \tag{45}$$

The linear displacements $\lambda_{10}^A, \lambda_{10}^B, \lambda_{10}^C$, and λ_{32}^C, and the angles $\varphi_{21}^A, \varphi_{21}^B, \varphi_{21}^C$ and φ_{43}^C are given by the following geometric *constraint conditions*:

$$\begin{aligned} &\vec{r}_{10}^A + a_{20}^T \vec{r}_{32}^A - a^T \vec{r}_{A3} = \vec{r}_0^P, \\ &\vec{r}_{10}^B + b_{20}^T \vec{r}_{32}^B - a^T \vec{r}_{B3} = \vec{r}_0^P, \\ &\vec{r}_{10}^C + c_{20}^T \vec{r}_{32}^C + c_{40}^T \vec{r}_4^P = \vec{r}_0^P, \end{aligned} \tag{46}$$

where one denotes

$$\begin{aligned} &\vec{r}_{10}^A = \begin{bmatrix} 0 \\ -R \\ \lambda_{10}^A \end{bmatrix}, \qquad \vec{r}_{10}^B = \begin{bmatrix} 0 \\ R \\ \lambda_{10}^B \end{bmatrix}, \\ &\vec{r}_{10}^C = \begin{bmatrix} -L_3 \\ 0 \\ \lambda_{10}^C \end{bmatrix}, \qquad \vec{r}_{32}^C = \begin{bmatrix} L_2 \\ 0 \\ -\lambda_{32}^C \end{bmatrix}, \\ &\vec{r}_{32}^A = \vec{r}_{32}^B = R_2 \vec{u}_1, \qquad \vec{r}_{A3} = -\vec{r}_{B3} = -r\vec{u}_2, \\ &\vec{r}_4^P = -L_1 \vec{u}_1, \qquad h = \sqrt{R_2^2 - (R-r)^2}, \\ &\sin\alpha = \frac{R-r}{R_2}, \qquad \cos\alpha = \frac{h}{R_2}. \end{aligned} \tag{47}$$

There is only one inverse geometric solution for the robot:

$$\begin{aligned} &R_2 \sin\left(\varphi_{21}^A + \alpha\right) = R - r + y_0^P, \\ &\lambda_{10}^A = z_0^P + R_2 \cos\left(\varphi_{21}^A + \alpha\right), \\ &R_2 \sin\left(\varphi_{21}^B + \alpha\right) = R - r - y_0^P, \\ &\lambda_{10}^B = z_0^P + R_2 \cos\left(\varphi_{21}^B + \alpha\right), \\ &L_2 \sin\left(\varphi_{21}^C + \alpha\right) = L_3 - L_1 \cos\phi, \\ &\lambda_{10}^C = z_0^P + L_1 \sin\phi + L_2 \cos\left(\varphi_{21}^C + \alpha\right), \\ &\lambda_{32}^C = y_0^P. \end{aligned} \tag{48}$$

6.2.2 *Velocities and accelerations*

The linear velocities $\vec{v}_{k0}^A$ $(k = 1, 2, \ldots, 6)$ of centers A_k of joints and the skew-symmetric matrices

$$\tilde{\omega}_{k0}^A = a_{k,k-1} \tilde{\omega}_{k-1,0}^A a_{k,k-1}^T + \omega_{k,k-1}^A \tilde{u}_3, \tag{49}$$

which are *associated* to absolute angular velocities given by (25), characterize the kinematics of the elements of each leg (for example, the leg A).

Equations of geometrical constraint, (42) and (46), can be derivate with respect to time to obtain the following *matrix conditions of connectivity* established for the relative angular velocities:

$$\begin{aligned} &v_{10}^A \vec{u}_i^T \vec{u}_3 + \omega_{21}^A R_2 \vec{u}_i^T a_{20}^T \tilde{u}_3 \vec{u}_1 = \vec{u}_i^T \dot{\vec{r}}_0^P, \\ &v_{10}^B \vec{u}_i^T \vec{u}_3 + \omega_{21}^B R_2 \vec{u}_i^T b_{20}^T \tilde{u}_3 \vec{u}_1 = \vec{u}_i^T \dot{\vec{r}}_0^P \quad (i = 2, 3), \\ &v_{10}^C \vec{u}_j^T \vec{u}_3 + \omega_{21}^C \left\{ L_1 \vec{u}_j^T c_{20}^T \tilde{u}_3 c_{32}^T c_{43}^T \vec{u}_2 + \vec{u}_j^T c_{20}^T \tilde{u}_3 \vec{r}_{32}^C \right\} \\ &\quad - v_{32}^C \vec{u}_j^T c_{20}^T \vec{u}_3 + \omega_{43}^C L_1 \vec{u}_j^T c_{40}^T \tilde{u}_3 \vec{u}_1 = \vec{u}_j^T \dot{\vec{r}}_0^P \\ &\quad (j = 1, 2, 3), \\ &\omega_{43}^C = \omega_{21}^C + \dot{\theta}. \end{aligned} \tag{50}$$

Equation (50) offers a closed-form matrix for the velocities $v_{10}^A, v_{10}^B, v_{10}^C, \omega_{21}^A, \omega_{21}^B, \omega_{21}^C, v_{32}^C, \omega_{43}^C$ and the *complete* Jacobian matrix of the robot as functions of *translation velocity* of the platform.

The above constraint (46) of the robot can be written as follows:

$$\left(R - r + y_0^P\right)^2 + \left(\lambda_{10}^A - z_0^P\right)^2 = R_2^2,$$

$$\begin{aligned}&\left(R-r-y_0^P\right)^2+\left(\lambda_{10}^B-z_0^P\right)^2=R_2^2,\\&\left(\lambda_{10}^C-z_0^P-L_1\sin\phi\right)^2+(L_3-L_1\cos\phi)^2=L_2^2.\end{aligned}\tag{51}$$

The derivative with respect to time of (51) leads to the matrix equation

$$J_1\dot{\vec{\varphi}}_{10}=J_2\begin{bmatrix}\dot{\phi} & \dot{y}_0^P & \dot{z}_0^P\end{bmatrix}^T.\tag{52}$$

Matrices J_1 and J_2 constitute the inverse and forward Jacobian of the new spatial parallel robot and can be expressed as

$$\begin{aligned}&J_1=\operatorname{diag}\{\delta_A \quad \delta_B \quad \delta_C\},\\&J_2=\begin{bmatrix}\beta_1^A & \beta_2^A & \beta_3^A\\ \beta_1^B & \beta_2^B & \beta_3^B\\ \beta_1^C & \beta_2^C & \beta_3^C\end{bmatrix},\end{aligned}\tag{53}$$

with

$$\begin{aligned}&\delta_A=\lambda_{10}^A-z_0^P,\\&\delta_B=\lambda_{10}^B-z_0^P,\\&\delta_C=\lambda_{10}^C-z_0^P-L_1\sin\phi,\\&\beta_1^A=0,\qquad \beta_2^A=-R+r-y_0^P,\\&\beta_3^A=\lambda_{10}^A-z_0^P,\\&\beta_1^B=0,\qquad \beta_2^B=R-r-y_0^P,\qquad \beta_3^B=\lambda_{10}^B-z_0^P,\\&\beta_1^C=L_1\left[\left(\lambda_{10}^C-z_0^P\right)\cos\phi-L_3\sin\phi\right],\\&\beta_2^C=0,\qquad \beta_3^C=\lambda_{10}^C-z_0^P-L_1\sin\phi.\end{aligned}\tag{54}$$

Let us assume that the robot has a virtual motion determined by the velocities $v_{10c}^{Cv}=1$, $v_{10c}^{Av}=0$, and $v_{10c}^{Bv}=0$. Characteristic virtual velocities are given by the connectivity conditions (50).

Again, the relative accelerations γ_{10}^A, γ_{10}^B, γ_{10}^C, ε_{21}^A, ε_{21}^B, ε_{21}^C, γ_{32}^C and ε_{43}^C of the components of this robot are given by some new connectivity conditions, which are obtained from the time derivative of (50). The following relations' results can be obtained:

$$\begin{aligned}&\gamma_{10}^A\vec{u}_i^T\vec{u}_3+\varepsilon_{21}^A R_2\vec{u}_i^T a_{20}^T\tilde{u}_3\vec{u}_1\\&\quad=\vec{u}_i^T\ddot{\vec{r}}_0^P-\omega_{21}^A\omega_{21}^A R_2\vec{u}_i^T a_{20}^T\tilde{u}_3\tilde{u}_3\vec{u}_1,\\&\gamma_{10}^B\vec{u}_i^T\vec{u}_3+\varepsilon_{21}^B R_2\vec{u}_i^T b_{20}^T\tilde{u}_3\vec{u}_1\\&\quad=\vec{u}_i^T\ddot{\vec{r}}_0^P-\omega_{21}^B\omega_{21}^B R_2\vec{u}_i^T b_{20}^T\tilde{u}_3\tilde{u}_3\vec{u}_1\quad(i=2,3),\\&\gamma_{10}^C\vec{u}_j^T\vec{u}_3+\varepsilon_{21}^C\left\{L_1\vec{u}_j^T c_{20}^T\tilde{u}_3c_{32}^T c_{43}^T\vec{u}_2+\vec{u}_j^T c_{20}^T\tilde{u}_3\vec{r}_{32}^C\right\}\\&\qquad-\gamma_{32}^C\vec{u}_j^T c_{20}^T\vec{u}_3+\varepsilon_{43}^C L_1\vec{u}_j^T c_{40}^T\tilde{u}_3\vec{u}_1\\&\quad=\vec{u}_i^T\ddot{\vec{r}}_0^P-\omega_{21}^C\omega_{21}^C\left\{\vec{u}_j^T c_{20}^T\tilde{u}_3\tilde{u}_3\vec{r}_{32}^C\right.\\&\qquad\left.+L_1\vec{u}_j^T c_{20}^T\tilde{u}_3\tilde{u}_3c_{32}^T c_{43}^T\vec{u}_2\right\}\\&\qquad-\omega_{43}^C\omega_{43}^C L_1\vec{u}_j^T c_{40}^T\tilde{u}_3\tilde{u}_3\vec{u}_2\\&\qquad-2\omega_{21}^C\omega_{43}^C L_1\vec{u}_j^T c_{20}^T\tilde{u}_3c_{32}^T c_{43}^T\tilde{u}_3\vec{u}_2\quad(j=1,2,3),\\&\varepsilon_{43}^C=\varepsilon_{21}^C+\ddot{\theta}.\end{aligned}\tag{55}$$

Equations (50) and (55) represent *the inverse kinematical model* of the parallel robot.

6.2.3 Dynamics simulation

In the inverse dynamical problem, by using of the general principle of virtual powers, some recursive matrix relations for the torques of three active systems are established.

The motion of the movable platform is controlled by three independent pneumatic systems that generate three forces

$$\begin{aligned}&\vec{f}_{10}^A=f_{10}^A\vec{u}_3,\qquad \vec{f}_{10}^B=f_{10}^B\vec{u}_3\quad\text{and}\\&\vec{f}_{10}^C=f_{10}^C\vec{u}_3\end{aligned}\tag{56}$$

which train the sliders on the guide-ways $A_1z_1^A$, $B_1z_1^B$, and Cz_1^C.

The wrench of the weight $m_k\vec{g}$ and the forces of inertia of an arbitrary rigid body T_k are determined with respect to the center A_k of a joint.

Knowing the kinematics state of each link, as well as all external forces acting on the robot, the active forces required for a given motion of the moving platform, will be easily computed applying (19) and (20). The following compact matrix relation expresses the

force of the first actuator:

$$f_{10}^{A} = \vec{u}_3^{T}\{\vec{F}_1^{A} + \omega_{21a}^{Av}\vec{M}_2^{A} + \omega_{21a}^{Bv}\vec{M}_2^{B} + \omega_{21a}^{Cv}\vec{M}_2^{C} + v_{32a}^{Cv}\vec{F}_3^{C} + \omega_{43a}^{Cv}\vec{M}_4^{C}\}, \quad (57)$$

with the following recursive notations:

$$\begin{aligned}
\vec{F}_{k0}^{A} &= m_k^{A}\left[\vec{\gamma}_{k0}^{A} + (\tilde{\omega}_{k0}^{A}\tilde{\omega}_{k0}^{A} + \tilde{\varepsilon}_{k0}^{A})\vec{r}_k^{CA}\right] - \vec{f}_k^{*A},\\
\vec{M}_{k0}^{A} &= m_k^{A}\tilde{r}_k^{CA}\vec{\gamma}_{k0}^{A} + \hat{J}_k^{A}\vec{\varepsilon}_{k0}^{A} + \tilde{\omega}_{k0}^{A}\hat{J}_k^{A}\vec{\omega}_{k0}^{A} - \vec{m}_k^{*A},\\
\vec{F}_k^{A} &= \vec{F}_{k0}^{A} + a_{k+1,k}^{T}\vec{F}_{k+1} \quad (k = 2, 1),\\
\vec{M}_k^{A} &= \vec{M}_{k0}^{A} + a_{k+1,k}^{T}\vec{M}_{k+1} + \tilde{r}_{k+1,k}^{T}a_{k+1,k}^{T}\vec{F}_{k+1}.
\end{aligned} \quad (58)$$

As the application, let us consider a spatial robot that has the following characteristics: $\phi^* = \pi/15$, $y_0^{G*} = 0.04$ m, $z_0^{G*} = 0.08$ m, $\Delta t = 6$ s, $L_1 = r = 0.1$ m, $L_3 = R = 0.25$ m, $L_2 = R_2 = L = 0.4$ m, $m_1 = 0.9751$ kg, $m_2 = 0.9803$ kg, $m_4 = 8.1573$ kg,

$$\hat{J}_2 = \begin{bmatrix} 0.0006 & & \\ & 0.0524 & \\ & & 0.0524 \end{bmatrix},$$

$$\hat{J}_4 = \begin{bmatrix} 0.0658 & & \\ & 0.0269 & \\ & & 0.0501 \end{bmatrix}.$$

Finally, we obtain the graphs of time-history of the active forces f_{10}^{A} (Fig. 9), f_{10}^{B} (Fig. 10), f_{10}^{C} (Fig. 11) of the three actuators.

7 Conclusions

A new dynamic analysis method based on the fundamental principle of virtual powers is introduced in this paper. Two examples, which are two 3-DOF parallel robots, are given as applications of the method. The matrix equations for the real-time computation of position, velocity and acceleration of each link of the robots can be established. Knowing all external forces acting on the robots, the forces required at the actuators in a given motion of the moving platforms will easily be computed applying the compact matrix equations. In the context of automatic control, the iterative matrix relations given in the inverse dynamics modeling can be easily transformed into a robust model for the computerized command of a robot. The methodology developed in this paper can be available for kine-

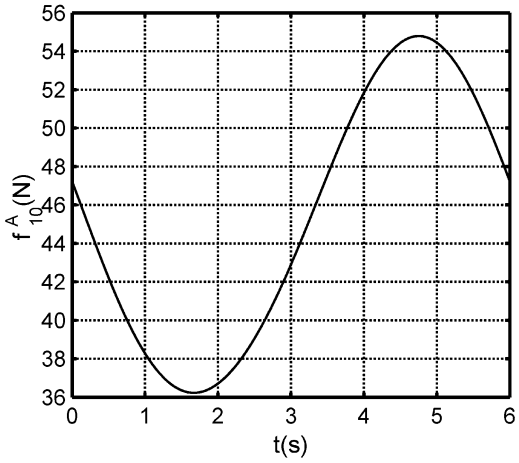

Fig. 9 Force f_{10}^{A} of the first actuator

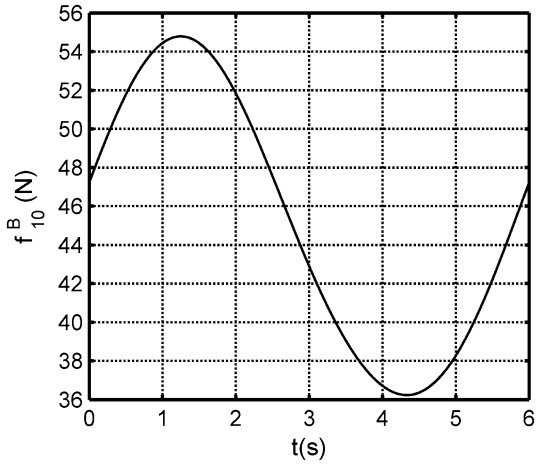

Fig. 10 Force f_{10}^{B} of the second actuator

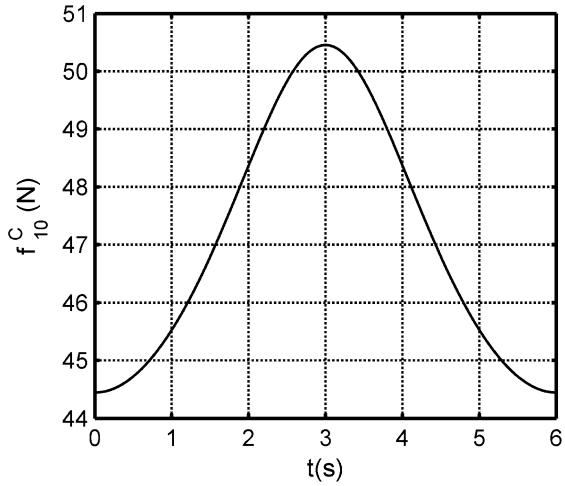

Fig. 11 Force f_{10}^{C} of the third actuator

matics analysis and nonlinear dynamics of a multi-body systems consisting of interconnected rigid and, eventually, deformable bodies.

Acknowledgements This work was supported in part by the National Natural Science Foundation of China under Grants Nos. 50505023 and 50775118, High Technology Research and Development Program (863 Program) of China (No. 2006AA04Z227) and the National Basic Research Program (973 Program) of China (No. 2007CB714000).

References

1. Tsai, L.-W.: Robot Analysis: The Mechanics of Serial and Parallel Manipulator. Wiley, New York (1999)
2. Chablat, D., Wenger, P.: Architecture optimisation of a 3-DOF parallel mechanism for machining applications: the orthoglide. IEEE Trans. Robot. Autom. **19**(3), 403–410 (2003)
3. Liu, X.-J., Wang, J., Gao, F., Wang, L.-P.: On the analysis of a new spatial three degrees of freedom parallel manipulator. IEEE Trans. Robot. Autom. **17**(6), 959–968 (2001)
4. Reboulet, C., Pigeyre, R.: Hybrid control of a 6-DOF in-parallel actuated micro-manipulator mounted on a Scara robot. In: Proceedings of the International Symposium on Robotics and Manufacturing: Research, Education and Applications, Burnaby, Canada, pp. 293–298 (1990)
5. Valenti, M.: Machine tools get smarter. ASME Mech. Eng. **17**, 70–75 (1995)
6. Cleary, K., Brooks, T.: Kinematics analysis of a novel 6-DOF parallel manipulator. In: Proceedings of the IEEE International Conference on Robotics and Automation, Texas, pp. 708–713 (1993)
7. Angeles, J.: Fundamentals of Robotic Mechanical Systems: Theory, Methods and Algorithms. Springer, New York (1997)
8. Carricato, M., Parenti-Castelli, V.: Singularity-free fully-isotropic translational parallel mechanisms. Int. J. Robot. Res. **21**(2), 161–164 (2002)
9. Parenti-Castelli, V., Di Gregorio, R.: A new algorithm based on two extra-sensors for real-time computation of the actual configuration of generalized Stewart–Gough manipulator. J. Mech. Des. **122**, 294–298 (2000)
10. Stewart, D.: A platform with six degrees of freedom. Proc. Inst. Mech. Eng. 1 **180**(15), 371–386 (1965)
11. Clavel, R.: Delta: a fast robot with parallel geometry. In: Proceedings of 18th International Symposium on Industrial Robots, Lausanne (1988)
12. Staicu, S., Carp-Ciocardia, D.C.: Dynamic analysis of Clavel's delta parallel robot, In: Proceedings of the IEEE International Conference on Robotics & Automation ICRA'2003, Taipei, Taiwan, pp. 4116–4121 (2003)
13. Tsai, L.-W., Stamper, R.: A parallel manipulator with only translational degrees of freedom. In: ASME Design Engineering Technical Conferences, Irvine, CA (1996)
14. Hervé, J.-M., Sparacino, F.: Star. A new concept in robotics. In: Proceedings of the Third International Workshop on Advances in Robot Kinematics, Ferrara (1992)
15. Gosselin, C., Angeles, J.: The optimum kinematics design of spherical three-degrees-of-freedom parallel manipulator. ASME J. Mech. Trans. Autom. Des. **111**(2), 202–207 (1989)
16. Li, Y.-W., Wang, J., Wang, L.-P., Liu, X.-J.: Inverse dynamics and simulation of a 3-DOF spatial parallel manipulator. In: Proceedings of the IEEE International Conference on Robotics & Automation, Taipei, Taiwan, pp. 4092–4097 (2003)
17. Dasgupta, B., Mruthyunjaya, T.S.: A Newton–Euler formulation for the inverse dynamics of the Stewart platform manipulator. Mech. Mach. Theory **34**, 1135–1152 (1998)
18. Kane, T.R., Levinson, D.A.: Dynamics, Theory and Applications. McGraw-Hill, New York (1985)
19. Sorli, M., Ferarresi, C., Kolarski, M., Borovac, B., Vucobratovic, M.: Mechanics of Turin parallel robot. Mech. Mach. Theory **32**(1), 51–77 (1997)
20. Geng, Z., Haynes, L.S., Lee, J.D., Carroll, R.L.: On the dynamic model and kinematics analysis of a class of Stewart platforms. Robot. Autonom. Syst. **9**, 237–254 (1992)
21. McCarthy, J.M.: Dual orthogonal matrix in manipulator kinematics. Int. J. Robot. Res. **5**(2), 45–51 (1986)
22. Staicu, S.: Mecanica teoretica. Edit. Didactica & Pedagogica, Bucharest (1998)
23. Staicu, S.: Inverse dynamics of a planetary gear train for robotics. Mech. Mach. Theory **43**, 918–927 (2008)
24. Staicu, S., Zhang, D., Rugescu, R.: Dynamic modelling of a 3-DOF parallel manipulator using recursive matrix relations. Robotica **24**(1), 125–130 (2006)
25. Guégan, S., Khalil, W., Chablat, D., Wenger, P.: Modélisation dynamique d'un robot parallèle à 3-DDL: l'Orthoglide. In: Conférence Internationale Francophone d'Automatique, Nantes, France, 8–10 Juillet (2002)
26. Merlet, J.-P.: Parallel Robots. Kluwer Academic, Dordrecht (2000)
27. Miller, K., Clavel, R.: The Lagrange-based model of delta-4 robot dynamics. Robotersysteme **8**, 49–54 (1992)
28. Staicu, S., Zhang, D.: A novel dynamic modelling approach for parallel mechanisms analysis. Robot. Comput.-Integr. Manuf. **24**, 167–172 (2008)
29. Staicu, S., Liu, X.-J., Wang, J.: Inverse dynamics of the HALF parallel manipulator with revolute actuators. Nonlinear Dyn. **50**, 1–12 (2007)
30. Tsai, L.-W.: Solving the inverse dynamics of Stewart–Gough manipulator by the principle of virtual work. ASME J. Mech. Des. **122**, 3–9 (2000)
31. Zhang, C.-D., Song, S.-M.: An efficient method for inverse dynamics of manipulators based on virtual work principle. J. Robot. Syst. **10**(5), 605–627 (1993)
32. Liu, X.-J., Jeong, J., Kim, J.: A three translational DoFs parallel cube-manipulator. Robotica **21**(6), 645–653 (2003)
33. Staicu, S.: Relations matricielles de récurrence en dynamique des mécanismes. Rev. Roum. Sci. Tech. Sér. Méc. Appl. **50**(1–3), 15–28 (2005)